



Strathprints Institutional Repository

Trines, Raoul M. G. M. and Murphy, C.D. and Bingham, Robert and Mendonca, Jose Tito and Norreys, P.A. and Reitsma, Albert (2004) *Numerical studies of photon acceleration in laser wakefields*. In: STFC Central Laser Facility Annual Report 2004/05. STFC, Swindon, pp. 85-86.

Strathprints is designed to allow users to access the research output of the University of Strathclyde. Copyright © and Moral Rights for the papers on this site are retained by the individual authors and/or other copyright owners. You may not engage in further distribution of the material for any profitmaking activities or any commercial gain. You may freely distribute both the url (<http://strathprints.strath.ac.uk/>) and the content of this paper for research or study, educational, or not-for-profit purposes without prior permission or charge.

Any correspondence concerning this service should be sent to Strathprints administrator: <mailto:strathprints@strath.ac.uk>

Numerical studies of photon acceleration in laser wakefields

R M G M Trines, C D Murphy, R Bingham, J T Mendonça, P A Norreys

Central Laser Facility, CCLRC Rutherford Appleton Laboratory, Chilton, Didcot, Oxon., OX11 0QX, UK

A J W Reitsma

Department of Physics, University of Strathclyde, Rottenrow, Glasgow, G4 0NG, UK

Main contact email address: r.trines@rl.ac.uk

Introduction

The concept of photon acceleration can be used to describe the spectral changes experienced by electromagnetic waves when they propagate in spatially and temporally varying plasmas¹. When the space and time scales of the plasma perturbations are much larger than the photon wavelength and period, geometric optics can be used to describe the motion of the electromagnetic wave-packets². Photons can exchange energy with the plasma through the action of the ponderomotive force. In particular, light travelling amidst a co-propagating region of temporally decreasing (increasing) plasma density will experience a redshift (blueshift). In this case, the photon picture can be used to describe the decrease (increase) in photon energy³. Photon acceleration due to relativistic ionization fronts is well documented experimentally, for microwaves⁴, as well as for light in the visible and near-infrared⁵⁻⁷. It has also been studied as a diagnostic tool for laser wakefields⁸.

When photon acceleration occurs during laser-plasma interaction, the following spectral characteristics can be observed. First of all, there is an asymmetric shift around the central frequency. The bulk of the pulse's photons shift a small distance towards the red side, because they lose energy while driving the wakefield. A smaller fraction of the photons shift a large distance towards the blue side. This is different from the case of ionization blueshift, in which the complete spectrum shifts towards the blue side, and over smaller distances^{6, 9}. There is a visible decrease of the intensity of the blueshifted tail with increasing plasma density, which is again something that one would not observe with ionization-induced blueshift. Also, the (redshifted) central peak in the spectrum is often split, with the two tips being separated by less than the plasma frequency.

Photon acceleration by wakefields is most obvious in experiments where the laser intensity is far beyond the ionization threshold for most of the interaction, such as the interaction of a multi-terawatt pulse with a narrow gas jet. Ionization blueshift is most obvious in experiments where the laser intensity is just above the threshold for most of the interaction, such as in the case of a laser pulse propagating through a gas-filled chamber, where it is out of focus most of the time⁹.

Theory

In order to study photon acceleration in laser-plasma interaction, simulations have been conducted using a photokinetic particle-in-cell (PIC) code³. This code uses the Wigner-Moyal description for the electromagnetic fields, in which the fields are described by the photon number density $N(t,x,k) = \epsilon(t,x,k)/\omega(k)$. Here ϵ denotes the energy density of the electromagnetic field and $\omega(k)$ is given by the linear dispersion relation for electromagnetic wave propagation. For the propagation of a laser pulse through a sufficiently underdense plasma, it can be shown that the total photon number is approximately conserved, leading to the following (Liouville) equation for $N(t,x,k)$ ²:

$$\frac{\partial N}{\partial t} + \frac{dx}{dt} \frac{\partial N}{\partial x} + \frac{dk}{dt} \frac{\partial N}{\partial k} = 0 \quad (1)$$

The factors dx/dt and dk/dt are obtained using ray-tracing equations from geometrical optics. Using the dispersion relation

for electromagnetic waves in plasma, $\omega^2 = c^2 k^2 + (e^2/\epsilon_0 m_e)(n/\gamma)$, we find $dx/dt = \partial\omega/\partial k = c^2 k/\omega$ and $dk/dt = -\partial\omega/\partial x = -(1/\omega) (e^2/\epsilon_0 m_e) \partial(n/\gamma)/\partial x$. Here, γ denotes the relativistic Lorentz factor due to plasma electron motion. Approximating N by a large number of macro-particles, where each macro-particle represents a fixed number of photons, the above equations allow one to follow the evolution of N by means of a kinetic model, in which the motion of each macro-particle is governed by ray-tracing equations.

For laser-induced wakefield generation without plasma electron self-trapping and negligible plasma heating, it is sufficient to use a non-linear relativistic cold-fluid model to describe the plasma motion. In this model, plasma perturbations are driven by the laser ponderomotive force¹⁰:

$$F_p = -\frac{m_e c^2}{2\gamma} \nabla \left(\frac{eA}{m_e c} \right)^2; \quad A^2 = \int \frac{d^3 k}{(2\pi)^3} \frac{N(t,x,k)}{\omega(k)} \quad (2)$$

Assuming that the transverse electron motion is dominated by the fast quiver motion in the laser field, while the longitudinal motion is dominated by the slow wake-field oscillations, we find that $\gamma = \sqrt{1 + p_x^2 + \langle A^2 \rangle}$ and $F_p = -(1/2\gamma) \nabla \langle A^2 \rangle$, angular brackets

denoting the average over the fast laser oscillations, and the one-dimensional electron fluid equations (with static ions) reduce to:

$$\begin{aligned} \frac{\partial n}{\partial t} + \frac{\partial (np_x/\gamma)}{\partial x} &= 0 \\ \frac{\partial p_x}{\partial t} + \frac{\partial \gamma}{\partial x} &= -E \\ \frac{\partial E}{\partial x} &= 1 - n \end{aligned} \quad (3)$$

Equations (1)-(3) allow us to describe the excitation of a wakefield by a laser pulse propagating through a plasma in a self-consistent way. Computer simulations based on these equations have been conducted, and the results are discussed below. The choice of parameters for the simulations has been inspired by the ‘‘dream beam’’ experiments that ultimately led to the first observation ever of a mono-energetic bunch of electrons accelerated to about 100 MeV in a laser-induced plasma wave^{11, 12}. In accordance with these experiments, it has been assumed that the pulse travels through pre-ionised plasma for the entire duration of the interaction, removing the need to simulate the ionization.

Simulation results

Figure 1 shows the time history of the simulation phase space. The green dots denote the photon macro-particles at the beginning of the simulation. The red dots represent the photons after various propagation distances. The black line represents the generated wakefield density perturbation. Initially (Fig. 1a), a wakefield is generated with amplitude close to its predicted value for a non-linear plasma wave for the given initial intensity. As the pulse propagates through the plasma, photons at its front and centre, that drive the plasma wave, become decelerated. Photons at the back of the pulse do not take part in the excitation of the wake. However, being near the back of the wake wave bucket, these photons experience a time-dependent increase in the plasma density, resulting in an increase in their frequency. In the initial stage, this is seen as the spectrum splitting into two peaks around the

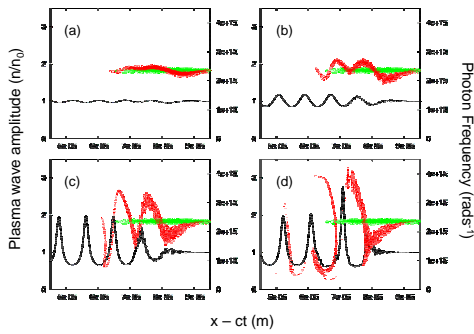


Figure 1. Phase space plot when the laser pulse has propagated a) 200 b) 500 c) 750 and d) 1000 μm in a plasma of density $3.6 \cdot 10^{19} \text{ cm}^{-3}$.

fundamental frequency (Figure 1a). The upshift of the photons continues to a greater extent at later times, resulting in the peak on the blue side being spread into a plateau.

The spectra produced after propagation of 750 μm for various densities is shown in Figure 2. At lower densities (not shown in Figure 2), the length of the first trough of the wake is such that only a few photons are eligible to be accelerated, and there is no significant blue-shifted plateau in the spectrum. When the density is increased, so that the length of the first wave bucket decreases, more of the tail of the laser pulse fits into the accelerating phase of the wave. This results in the number of accelerated photons increasing markedly.

For the range of densities used in our simulations, the pulse covers more than one plasma wave bucket, and as the plasma wave length changes with the square root of the density, the number of photons eligible for acceleration will not vary too much between the lowest and highest density used. However, since the rate of evolution of the pulse increases with increased density, one expects to see an increase in the maximum photon blueshift, i.e. in the spectral width of the blueshifted shoulder. As the total number of photons in the blueshifted shoulder does not vary much, an increase in spectral width must necessarily lead to a decrease in intensity of the shoulder. This is well reflected by the results from both simulations and experiments, where it can indeed be observed that the width of the blueshifted shoulder increases with increased density, while its intensity drops.

Simulation results exhibiting a split main laser peak are displayed in Figure 3, for a plasma background density of (a) $0.9 \cdot 10^{19} \text{ cm}^{-3}$ and (b) $1.9 \cdot 10^{19} \text{ cm}^{-3}$. While the density is lower than before, the laser intensity is higher, ($a_0 = 1.1$) in order to have a comparable lowest order evolution of the laser pulse while avoiding nonlinear saturation, which might confuse the picture. In both Figures, we see a frequency split in the transmitted light around ω_0 . This is the result of the laser modulational instability, which drives the wakefield and causes a 'wiggle' in the photon distribution which gets progressively larger towards the tail of the pulse. By this mechanism, the photons at the tail of the pulse are shifted beyond the 'split peak' stage and evolve into a shoulder. As the pulse propagates, photons at the head of the pulse, which were downshifted during production of the wake, are up- and down-shifted with respect to each other. Towards the end of the interaction, this 'wiggle' at the front of the pulse becomes larger than the laser bandwidth, allowing the 'split peak' to appear once more. The decreased plasma density causes non-linear saturation of the acceleration process to be postponed, leading to a cleaner photon spectrum after the interaction.

Conclusions

In conclusion, we have performed numerical studies of photon acceleration by laser-driven plasma waves. The three main features that distinguish this type of photon acceleration from

blueshift induced by ionization fronts are the asymmetric redshift/blueshift, the intensity decrease of the blueshifted tail with increasing plasma density, and the split fundamental peak. By means of photon kinetic numerical treatment, enhanced insight into the photon acceleration process could be gained, and the origin of the observed features uncovered. When coupled to experimental results, photon kinetics will prove to be a powerful diagnostic of large amplitude plasma waves, of significant interest to plasma-based laser acceleration schemes.

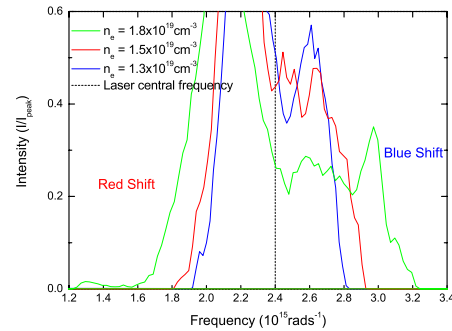


Figure 2. Simulation results showing the optical spectra as a function of plasma density. A decrease in blue-shift intensity is seen as the density increases.

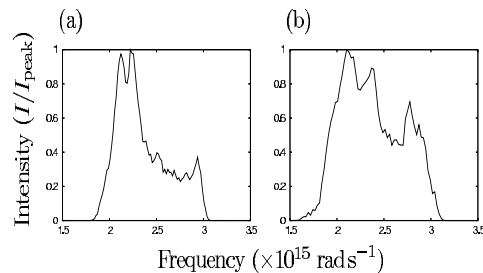


Figure 3. Examples of spectra exhibiting a split main peak, at a plasma density of (a) $0.9 \cdot 10^{19} \text{ cm}^{-3}$ and (b) $1.9 \cdot 10^{19} \text{ cm}^{-3}$. The central frequency is at $2.4 \cdot 10^{15} \text{ rad/s}$.

References

1. S.C. Wilks, J. M. Dawson, W. B. Mori, T. Katsouleas, M. E. Jones, Phys. Rev. Lett. **62**, 2600 (1989).
2. J.T. Mendonça, Theory of Photon Acceleration, (Institute of Physics Publishing, Bristol 2001).
3. L.O. Silva and J.T. Mendonça, Opt. Commun. **196**, 285 (2001).
4. R.L. Savage, C. Joshi and W.B. Mori, Phys. Rev. Lett. **68**, 946 (1992).
5. J.M. Dias *et al.*, Phys. Rev. Lett. **78**, 4773 (1997).
6. W. M. Wood, C. W. Siders, M. C. Downer, Phys. Rev. Lett. **67**, 3523 (1991).
7. N.C. Lopes *et al.*, Europhys. Lett. **66**, 371, (2004).
8. J.M. Dias, L.O. Silva and J.T. Mendonça, Phys. Rev. ST Accel. Beams **1**, 031301 (1999).
9. J.K. Koga *et al.*, Phys. Plasmas **7** 5223 (2000).
10. L. O. Silva, R. Bingham, J. M. Dawson, and W. B. Mori, Phys. Rev. E **59**, 2273 (1999).
11. S.P.D. Mangles *et al.*, Nature **431**, 535 (2004).
12. C.D. Murphy *et al.*, CLF Annual Report 2004/2005, p80